Barrier Engineering of Lattice Matched AlInGaN/ GaN Heterostructure Toward High Performance E-mode Operation

Niraj Man Shrestha
Department of Electrical and Computer Engineering and Center for mmWave Smart Radar System and Technologies, National Chiao Tung University, Hsinchu 30010, Taiwan
Email: nirajnctu@gmail.com

Chao-Hsuan Chen
Institute of Communications Engineering, National Chiao Tung University, Hsinchu 30010, Taiwan

Zuo-Min Tsai
Institute of Communications Engineering, Department of Electrical and Computer Engineering, and Center for mmWave Smart Radar System and Technologies, National Chiao Tung University, Hsinchu 30010, Taiwan

Yiming Li
Institute of Communications Engineering, Department of Electrical and Computer Engineering, and Center for mmWave Smart Radar System and Technologies, National Chiao Tung University, Hsinchu 30010, Taiwan
Email: ymli@faculty.nctu.edu.tw

Jenn-Hawn Tarng
Institute of Communications Engineering, Department of Electrical and Computer Engineering, and Center for mmWave Smart Radar System and Technologies, National Chiao Tung University, Hsinchu 30010, Taiwan

Seiji Samukawa
Center for mmWave Smart Radar System and Technologies, National Chiao Tung University, Hsinchu 30010, Taiwan and Institute of Fluid Science, Tohoku University, Sendai 980-8557, Japan

***Abstract*— Electrical characteristics of lattice matched AlInGaN/GaN high electron mobility transistors with different barrier engineering was studied theoretically by solving drift diffusion equation. The results of the study thoroughly disclose the mitigation of induced polarization charge on lowering Al and In content in barrier resulting in a positive shift of threshold voltage with huge deduction on drain current. The newly designed lattice match double $Al_{0.54}In_{0.12}Ga_{0.34}N$/ $Al_{0.18}In_{0.04}Ga_{0.78}N$ barrier recess gate HEMT helps to boost the drain current by reducing the access resistance and enhancing the polarization charge density. The proposed HEMT exalted current density and transconductance by two times with significant shift of threshold voltage in positive axis than that of single barrier structure. Conclusively, the high performance novel double barrier recess gate E-mode HEMT will be key for real and efficient high power switching application.**

Keywords—AlInGaN/GaN HEMT, Double barrier, recess gate, simulation, Physical models, Drift diffusion, lattice matched.

I. INTRODUCTION

AlGaN/GaN High Electron Mobility Transistor (HEMT) breathtaking performance has been made in the field of high-power and high-frequency electronic applications due to the existence of high-mobility two-dimensional electron gas (2DEG) at the AlGaN/GaN interface, large conduction band offset, and strong piezoelectric and spontaneous polarization effects. Performance of the device can be improved by increasing the Al content of the AlGaN barrier layer. However, significant drop in electron mobility (μ_e) for high aluminum composition than 30% in the barrier layer due to the onset of AlGaN relaxation has detrimental effect on performance of AlGaN/GaN HEMT [1]. In order to get rid of this problem, the AlGaN barrier is replaced by quaternary AlInGaN because the quaternary has wide range

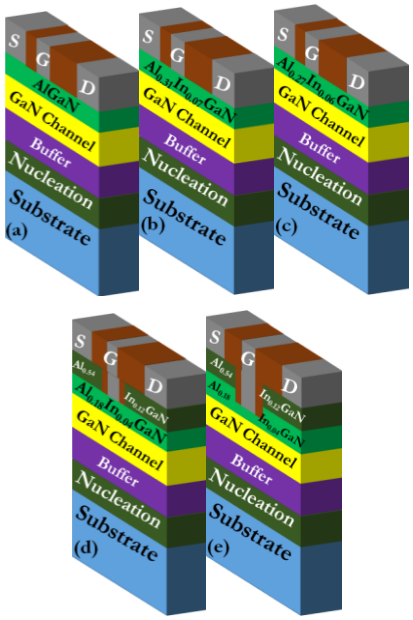

Fig. 1. The cross-sectional views of (a) conventional AlGaN/GaN HEMT, (b) $Al_{0.31}In_{0.07}Ga_{0.62}N$/GaN HEMT, (c) $Al_{0.27}In_{0.06}Ga_{0.67}N$/GaN HEMT, (d) $Al_{0.54}In_{0.12}Ga_{0.34}N$/ $Al_{0.18}In_{0.04}Ga_{0.78}N$/GaN HEMT, and (e) Recess gate $Al_{0.54}In_{0.12}Ga_{0.34}N$/ $Al_{0.18}In_{0.04}Ga_{0.78}N$/GaN HEMT.

of adjustments of the bandgap and lattice constant and suf ficiently large spontaneous polarization [2]. Researchers shift their interest to lattice-matched quaternary barrier layer grown to GaN due to spontaneous polarization-induced high-density 2DEG at AlInGaN/GaN heterojunction interface [1, 3-4] which facilitates to reduce strain-related defects on adjusting the different bandgap. Furthermore, the stronger polarization effect and higher mobility of AlInGaN

978-1-7281-0940-4/19/$31.00 ©2019 IEEE

TABLE I ADOPTED DEVICE PARAMETERS

Parameter \ Sample	Cal. Sample	I	II	III	IV
Channel Thickness (μm)	2	2	2	2	2
Recess Gate Depth (nm)	-	-	-	5	8
Al comp.(1st barrier) %	29	31	27	18	18
Al comp. (2nd barrier) %	-	-	-	54	54
Gate Length (μm)	3	0.16	0.16	0.16	0.16
Barrier Thickness (nm)	15.5	8.5	8.5	8.5	8.5
2nd Barrier Thickness (nm)	-	-	-	5	5
Indium Comp. (1st barrier) %	-	7	6	4	4
Indium Comp. (2nd barrier) %	-	-	-	12	12

for the same lattice strain as in AlGaN/GaN, help to boost the performance of the devices beyond the limit of ternary barrier layers. Moreover, use of AlInGaN as the barrier layer is beneficial to reduce the gate leakage current and to increase carrier mobility with increase of 2DEG density [5].

However, a higher 2DEG density induced at such heterointerface results the device operated in depletion mode [6]. Due to cost effective and safety issue, enhancement-mode (E-mode) devices are more desirable in the practical applications [7]. Several approaches have been popular to realize E-mode operation such as recess gate [8], fluoride implantation, p-type Gate [7] etc. However, these technologies include complicated fabrication procedures. Ketteniss *et al.* reported quaternary AlInGaN/GaN E-mode HEMT by using low Al-content in quaternary AlInGaN barrier [9]. Unfortunately, drastic reduction of current density limits the performance of the HEMT.

In this report, we have studied the effect of AlInGaN barrier engineering on threshold voltage (V_{th}) and reported lattice matched double barrier AlInGaN/GaN e-mode HEMT to boost the performance of the device.

II. DEVICE STRUCTURE & METHODOLOGY

To verify and validate the physical and transport model, simulation results were calibrated with experimental results from AlGaN/GaN HEMT device. The schematic cross-section of the AlGaN/GaN HEMT used for calibration is shown in Figure 1(a). The details of the HEMT which was used to examine the accuracy of simulation data are found in our previous report [8]. After calibration, new HEMTs structure are proposed and the proposed device are theoretically studied by using calibrated models. AlInGaN/GaN HEMT with the (Sample I), $Al_{0.27}In_{0.06}Ga_{0.67}N$ barrier (Sample II), $Al_{0.54}In_{0.12}Ga_{0.34}N$ /$Al_{0.18}In_{0.04}Ga_{0.78}N$ barriers with 5 nm recess gate (Sample III) and $Al_{0.54}In_{0.12}Ga_{0.34}N$/ $Al_{0.18}In_{0.04}Ga_{0.78}N$ double barrier with 8 nm recess (Sample IV), as shown in Figs. 1(b)-1(e), are the proposed structures for theoretical study of dc and transfer characteristics. The adopted parameters of studied device are listed in Table I.

The device characteristics are simulated by numerically solving 2D drift-diffusion (DD) transport model together with the strain generated polarization model [10], the high field saturation and the interface fixed charge at interface.

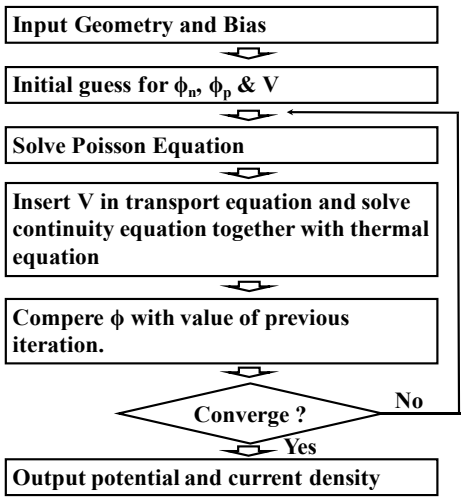

Fig. 2 Flowchart to solve the DD system

Additionally, mobility degradation due to impurity scattering are also properly modeled. To study HEMTs with recess gate structure, acoustic phonon scattering and surface roughness scattering are also taken into the account. Furthermore, the interface fixed charge at the interfaces between the AlGaN barrier layer and nitride layer and the acceptor buffer trap at GaN buffer are activated. The simulation flow of the device is shown in Fig. 2.

III. RESULTS AND DISCUSSION

It is noted that AlInGaN barriers used in this study were latticed matched with GaN. The calculated Al, In and Ga composition for latticed matched AlInGaN with GaN are plotted in Fig. 3(a).

The perfectly overlapping simulated and measured transfer (at V_D = 5 V) of AlGaN/GaN HEMT with nearly equal V_{th} and maximum transconductance ($G_{m,max}$) as shown in Fig. 3(b) reveal that the transport and physical models solved during simulation exactly defined the physical phenomenon. The accuracy of the physical and transport models is further verified by perfectly matched simulated dc characteristics with measured outcomes for different gate voltages as shown in Fig. 3(c).

The transfer characteristics and G_m of the lattice matched AlInGaN/GaN HEMT for different barrier engineering as shown in Figs. 3(d) and 3(e) reveal that both current density ($I_{D,max}$) and $G_{m,max}$ of device shrink with positive shift of V_{th} on decreasing Al composition in the AlInGaN barrier from 0.31 to 0.27. Furthermore, it is observed that the HEMT with double $Al_{0.54}In_{0.12}Ga_{0.34}N$/ $Al_{0.18}In_{0.04}Ga_{0.78}N$ barriers with 5 nm recess (Sample III) in gate region offer $I_{D,max}$ and G_m of 768 mA/mm and 493 mS/mm respectively which are lower in comparison of sample I and sample II. Moreover, sample III was redesigned with increasing recess depth 8 nm, $I_{D,max}$ was reduced to 688 mA/mm and G_m is increased to 558 mS/mm with significant increase of V_{th} toward the positive direction. Strong polarization induced interface charge at heterointerface is the key factor behind the excellent transfer properties of the proposed device with double AlInGaN barriers. It is found that the polarization induced interface charge (σ_{int}) is strongly depend on Al and In composition and is expressed as [11],

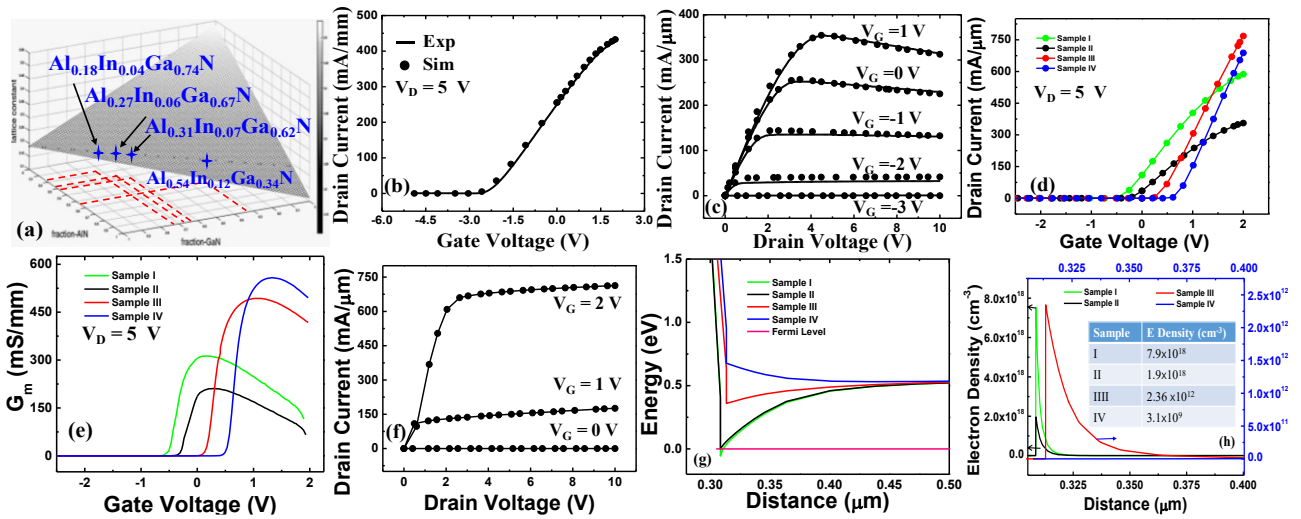

Fig. 3. Plot of (a) Calculated lattice matched $Al_xIn_yGa_zN$ with GaN, (b) measured and simulated transfer characteristics of calibrated sample at V_D = 5 V, (c) measured and simulated dc characteristics of calibrated sample, (d) I_D -V_G characteristics of AlInGaN/GaN HEMTs, (e) G_m of AlInGaN/GaN HEMTs, (f) transfer characteristics of sample IV, (g) Conduction band profile, and (h) n_s distribution, in gate area of AlInGaN/ GaN HEMT under zero bias condition (cut vertically in gate region).

$$\sigma_{\text{int}} = P_{GaN} - P_{InAlGaN} = P_{sp}^{GaN} - x \cdot P_{sp}^{AlN}, \quad (1)$$
$$- y \cdot P_{sp}^{InN} - z \cdot P_{sp}^{GaN} - b_{AlGaN}\, x \cdot z$$
$$- b_{InGaN} \cdot y \cdot z - b_{InAlN} \cdot x \cdot y - P_{pz}^{InAlGaN}$$

where P_{sp} and P_{pz} are spontaneous and piezoelectric polarization of respective binary compound and b_{AlGaN}, b_{InGaN} and b_{AlInN} are bowing parameters for ternary nitrides and are calculated by using following expression [12],

$$b_{AlGaN} = 4P_{sp}^{AlGaN} - 2\left(P_{sp}^{AlN} + P_{sp}^{GaN}\right), \quad (2)$$

$$b_{InGaN} = 4P_{sp}^{InGaN} - 2\left(P_{sp}^{InN} + P_{sp}^{GaN}\right), \quad (3)$$

$$b_{AlInN} = 4P_{sp}^{AlInN} - 2\left(P_{sp}^{AlN} + P_{sp}^{InN}\right), \quad (4)$$

Spontaneous polarization of ternary compound can be calculated by [12]

$$P_{sp}^{AlGaN} = -0.09x - 0.034(1-x) + 0.021x(1-x), \quad (5)$$

$$P_{sp}^{InGaN} = -0.042x - 0.034(1-x) + 0.037x(1-x), \quad (6)$$

$$P_{sp}^{AlInN} = -0.09x - 0.042(1-x) + 0.07x(1-x), \quad (7)$$

Since AlInGaN barrier layer are lattice matched with GaN, strain induced piezoelectric polarization was neglected in simulation. Therefore, effective polarization induced interface charge (σ_{int}) is expressed as,

$$\sigma_{\text{int}} = P_{GaN} - P_{InAlGaN} = P_{sp}^{GaN} - x \cdot P_{sp}^{AlN}$$
$$- y \cdot P_{sp}^{InN} - z \cdot P_{sp}^{GaN} - b_{AlGaN} x \cdot z \quad (8)$$
$$- b_{InGaN} \cdot y \cdot z - b_{InAlN} \cdot x \cdot y,$$

And, similarly, 2DEG density (n_s) is a function of interface charge and is given by [11]

$$n_s = \frac{\sigma_{\text{int}}}{q} - \frac{\varepsilon_0 \varepsilon_r}{q^2 d}\left(q\phi_b - \Delta - \Delta E_c\right), \quad (9)$$

where d is the barrier thickness, ΔE_c is the conduction band offset and Δ is the penetration of the conduction band below the Fermi level at the heterointerface. Conduction band energy profile at zero biased condition as shown in Fig. 3(g) suggests that comparatively smaller ΔE_c is observed for low Al composition barrier and further decrease on increasing recess depth. Due to combined effect of σ_{int} and small ΔE_c, sample II has smaller n_s than that of sample I as listed in Table II. Notably, high Al composition of lattice matched second barrier of sample III and sample IV result high induced spontaneous polarization charge at the interface [12] which results in improvement of n_s significantly (Table II). Therefore, larger current density observed for Sample III than that of Sample I and Sample II whereas large positive threshold voltage is due to recess of second AlInGaN barrier beneath the gate region. Nonetheless, recess depth leads highly reduced n_s in gate region in sample III and sample IV as shown in Fig. 3 (h). Therefore, these samples offer large positive threshold voltages along with large current density. Notably, high effective potential to the channel, increased parasitic resistances, and deep level traps in barrier due to recess depth, small current density is observed in sample III and sample IV [8]. The dc characteristics of sample IV is shown in Fig. 3(f). The current flow across 2DEG in conventional HEMT devices (Sample I and Sample II) shown in Fig. 4(a) revels that there is single current flowing path in normal HEMT structure. However, there are two paths for current flow in proposed double barrier HEMT (Sample IV); one is along $Al_{0.18}In_{0.04}Ga_{0.78}N$/GaN interface and the other is along $Al_{0.54}In_{0.12}Ga_{0.34}N$/$Al_{0.18}In_{0.04}Ga_{0.78}N$ as shown in Fig 4 (b) which is similar to the resistors combined parallel where effective resistance is decreased [14]. The upper channel is cut by the recess gate and the electrons don't have enough energy to overcome the potential barrier and so they pass from the top channel. The decrease in effective resistance of the channel helps to enhance the current density of the device. The second channel contributes to the total current. The equivalent circuit for double-channel HEMT [15] is shown in Fig. 4(c). The lattice matched $Al_{0.54}In_{0.12}Ga_{0.34}N$ /$Al_{0.18}In_{0.04}Ga_{0.78}N$ /GaN recess gate HEMT shows unexpectedly better output performance with significantly large $I_{D,max}$ and G_m, and the performance with significantly large $I_{D,max}$ and G_m, and

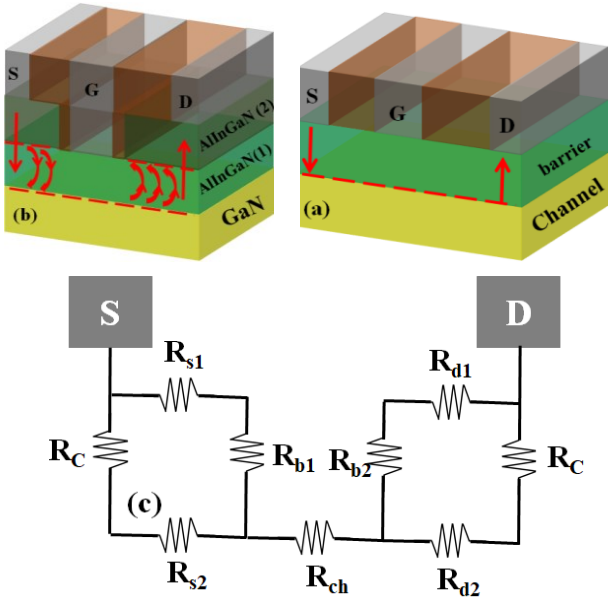

Fig.4. Schematic of the current flow in the (a) Single barrier (b) double-barrier devices, and (c) Equivalent circuit of the double-barrier HEMTs.

TABLE II COMPARISON OF OUR RESULTS WITH SIMILAR REPORTS

Sample	$I_{D,max}$ (mA/mm)	$G_{m,max}$ (mS/mm)	n_s (cm^{-3}) ($\times 10^{19}$)	V_{th} (V)
I	586	312	1.89	-0.5
II	356	210	1.02	-0.2
III	768	493	4.15	0.4
IV	688	558	4.15	0.7
Ref [16]	**338**	**165**	**-**	**0.2**

surprisingly large and positive V_{th} than previous report for e-mode AlGaInN/GaN HEMT as shown in Table II.

IV. CONCLUSION

Electrical properties of the different lattice matched AlInGaN/GaN HEMT were studied by using experimentally calibrated transport and physical models. Results observed that e-mode HEMT with low Al and In composition in AlInGaN barrier offer significant deduction of current density. The proposed novel double barrier recess gate HEMT gives surprisingly large current density with large positive V_{th} due to high polarization charge and low channel resistance. Finally, the high performance proposed e-mode will be advantageous for future high performance real high power high frequency application.

ACKNOWLEDGMENT

This work was supported in part by the Ministry of Science and Technology, Taiwan, under Grant MOST 106-2221-E-009-149, Grant MOST 106-2622-8-009-013-TM, Grant MOST 107-2622-8-009-011-TM, Grant MOST 107-2221-E-009-094, and Grant MOST 107-3017-F-009-001, in part by the "Center for mmWave Smart Radar Systems and Technologies" under the Featured Areas Research Center Program within the framework of the Higher Education Sprout Project by the Ministry of Education in Taiwan.

REFERENCES

[1] M. Gonschorek, J.-F. Carlin, E. Feltin, M. A. Py, and N. Grandjean, "High electron mobility lattice-matched AlInN/GaN field-effect transistor heterostructures," Appl. Phys. Lett. vol. 89, pp. 062106, August 2006.

[2] Y. Liu, H. Jiang, S. Arulkumaran, T. Egawa, B. Zhang, and H. Ishikawa, "Demonstration of undoped quaternary AlInGaN/GaN heterostructure field-effect transistor on sapphire substrate," Appl. Phys. Lett, vol. 86, pp 223510, May 2005.

[3] B. Reuters, A. Wille, B. Hollander, E. Saklauskas, N. Ketteniss, C. Mauder, R. Goldhahn, M. Heuken, H. Kalisch, and A. Vescan, "Growth Studies on Quaternary AlInGaN Layers for HEMT Application," J. Electron. Mater., vol. 41, pp. 905-909, March 2012.

[4] Y. Liu, T. Egawa, H. Jiang, B. Zhang, H. Ishikawa, and M. Hao, "Near-ideal Schottky contact on quaternary AlInGaN epilayer lattice-matched with GaN," Appl. Phys. Lett, vol.85, pp.6030, October 2004.

[5] N Ketteniss, L-R Khoshroo, M Eickelkamp1, M Heuken, H Kalisch, R H Jansen and A Vescan, "Study on quaternary AlInGaN/GaN HFETs grown on sapphire substrates," Semicond. Sci. Technol. Vol. 25, pp. 075013, May 2010.

[6] H. Hahn, B. Reuters, A Wille, N. Ketteniss, F. Benkhelifa, O. Ambacher, H. Kalisch, and A. Vescan, "First polarization-engineered compressively strained AlInGaN barrier enhancement-mode MISHFET," Semicond. Sci. Technol. vol. 27, pp. 055004, March 2012.

[7] N. M. Shrestha, Y. Li, and E. Y. Chang, "Step buffer layer of $Al_{0.25}Ga_{0.75}N/Al_{0.08}Ga_{0.92}N$ on P-InAlN gate normally-off high electron mobility transistors," Semicond. Sci. Technol., vol. 3, pp. 075006, June 2016.

[8] N. M. Shrestha, Y. Li, T. Suemitsu, and S. Samukawa, "Electrical Characteristic of AlGaN/GaN High-Electron-Mobility Transistors With Recess Gate Structure," IEEE Trans. Electron Devices, vol. 66, pp. 1694-1698, April 2019.

[9] N. Ketteniss, A. Askar, B. Reuters, A. Noculak, B. Hollander, H Kalisch, and A. Vescan, "Polarization-reduced quaternary InAlGaN/GaN HFET and MISHFET," Semicond. Sci. Technol., vol. 27, pp. 055012, April 2012.

[10] O. Ambacher, B. Foutz, J. Smart, J. R. Shealy, N. G. Weimann, K. Chu, M. Murphy, A. J. Sierakowski, W. J. Schaff, L. F. Eastman, R. Dimitrov, A. Mitchell, and M. Stutzmann, "Two dimensional electron gases induced by spontaneous and piezoelectric polarization in undoped and doped AlGaN/GaN heterostructures," *J. Appl. Phys.*, vol. 87, no. 1, pp. 334–344, December 2000.

[11] N. Ketteniss, L. R. Khoshroo, M. Eickelkamp, M. Heuken, H. Kalisch, R. H. Jansen and A. Vescan, "Study on quaternary AlInGaN/GaN HFETs grown on sapphire substrates," Semicond. Sci. Technol., vol. 2, pp. 075013, June 2010.

[12] D. Godwinraj, H. Pardeshi, S. K. Pati, N. Mohankumar, and C. K. Sarkar, "Polarization based charge density drain current and small-signal model for nano-scale AlInGaN/AlN/GaN HEMT devices," Superlattices Microstruct, vol. 54, pp. 188–203, December 2013.

[13] N. M. Shrestha, Y. Li, E. Y. Chang, "Optimal design of the multiple-apertures-GaN-based vertical HEMTs with SiO2 current blocking layer," J Comput Electron, vol. 15, pp. 154-162, March 2016.

[14] N. M. Shrestha, Y. Li, E. Y. Chang, "Optimal design of the multiple-apertures-GaN-based vertical HEMTs with SiO2 current blocking layer," J Comput Electron, vol. 15, pp. 154-162, March 2016.

[15] T. Palacios, A. Chini, D. Buttari, S. Heikman, A. Chakraborty, S. Keller, S. P. DenBaars, and U. K. Mishra, "Use of Double-Channel Heterostructures to Improve the Access Resistance and Linearity in GaN-Based HEMTs," *IEEE Trans. Electron Devices*, vol. 53, pp. 562-565, March 2006.

[16] B. Reuters, A. Wille, N. Ketteniss, H. Hahn, B. Hollander, M. Heuken, H. Kalisch, and A. Vescan, "Polarization-Engineered Enhancement-Mode High-Electron-Mobility Transistors Using Quaternary AlInGaN Barrier Layers," J. Electron. Mater., Vol. 42, pp. 826-832, February 2013.